Nonlinear Conductivity of Fullerenol Aqueous Solutions

Roberto B. Sardenberg, Carlos E. Teixeira, Mauricio Pinheiro, and José M. A. Figueiredo*

Departamento de Física, Universidade Federal de Minas Gerais, Caixa Postal 702, Belo Horizonte, MG-30.123-970, Brazil

ABSTRACT Fullerenols have been a subject of intense research in many fields with the claim of possible applications in biomedicine such as free-radical sponges, antioxidants, and photosensitizers. However, its transport characteristics, important in determining the feasibility of many applications, have not been studied yet. In this work, electrochemical impedance of aqueous solutions of two types of fullerenols ($C_{60}(OH)_{22-26}$ and $C_{60}(OH)_{18-22}(OK)_4$) was measured. Sample conductivity was extracted from impedance data, and a nonlinear concentration-dependent conductivity was found for one of two types ($C_{60}(OH)_{18-22}(OK)_4$). A concentration-dependent mobility that accounts electrophoretic and relaxation effects could explain experimental data. As a result, we obtained some fullerenol parameters, relevant to transport phenomena: its hydrodynamic radius, the number of attached hydroxides, and the number of counterions solvated into solution. In addition, an important result for pharmaceutical applications has been discussed, which is the change of pH in water induced by the different concentrations of fullerenol, indicating it behaves as a weak acid.

KEYWORDS: fullerenols · mobility · conductivity · Debye–Hückel theory · impedance spectroscopy

Fullerenes are a vast family of three-dimensional nanoscopic cage-like molecules with dozens of sp^2-hybridized carbon atoms arranged at the vertices of hexagons and pentagons. Since the discovery of the two most abundant fullerenes, the C_{60} and the C_{70}, in 1985 by Kroto *et al.*,[1] and their production in macroscopic quantities in 1991 by Krätschmer *et al.*,[2] these molecules have been attracting the attention of a large number of researchers from several areas from chemistry, to physics, medicine, and material sciences. Their potential applications range from hybrid photovoltaic cells,[3] molecular electronics[4] and spintronics[5] to biomedical applications. In the latter case, they can be used, for example, as drug carriers, antiviral drugs, X-ray and MRI contrasts, antioxidant drugs (against neurodegenerative disorders like Parkinson's and Alzheimer diseases), and photosensitizers for photodynamic therapy (PDT).[6] However, the major drawback for the applications of fullerenes as drugs is their negligible solubility in water. Several strategies have been proposed to overcome this problem without making the fullerenes lose their properties of interest for certain drugs like, for example, their cage-like structure, their large number of unsaturated bonds, and their optical properties. Some of these strategies[7] are based either on exohedral functionalization of the carbon cage with polar groups (*e.g.*, −OH, −COOH, *etc.*) or on supermolecular chemistry involving cyclodextrins and polymers. Among the several methods to obtain water-soluble functionalized fullerenes, the binding of several −OH groups resulting in molecules known as fullerenols or poly(hydroxy)-fullerenes ($C_{60}(OH)_x$ where x is the number of −OH groups) as well as fullerenol salts ($[C_{60}(OH)_xO_y]^-[K,Na^+]_y$), is the most simple.[8−11] For that, the most common method is based on the phase transfer of fullerenes from an organic solution (benzene or toluene as solvents) to an alkaline aqueous solution (NaOH or KOH) where the polyhydroxylation occurs. Phase-transfer catalysts such as tetrabutylammonium hydroxide (TBAH) and poly(ethylene glycol) (PEG) are usually employed.[12] Depending on the reaction conditions, one may obtain fullerols with a number of attached hydroxyls varying from 16 to 32 groups.[8−13] The interest in the synthesis as well as in the structure of fullerenols is not only justified because of its fundamental properties but also due to their recently verified free-radical scavenging properties.[14−16] These properties make the fullerenol an excellent antioxidant and a potential drug for many illnesses that are somehow associated with free radicals, such as ischemias,[17] radiation sickness induced by radiotherapy against cancer,[18−20] among others.

On the other hand, very little is known about the electrochemical properties of different fullerenols in water, such as the conductivity of the solutions as a function of the concentration, their dissociation, the ion/contra-ion equilibrium, and the fullerenol hydrodynamic radius. These properties are fundamental for the investigation and

* Address correspondence to josef@fisica.ufmg.br.

Received for review October 27, 2010 and accepted March 9, 2011.

Published online March 09, 2011
10.1021/nn102913p

the design of novel fullerenol-based pharmaceuticals, either for use in PDT or as antioxidants, because they are directly related to the mobility and the diffusion of the fullerenol ion in aqueous/biological medium, as well as the pH and p*K* changes induced in this medium by the dissociation of these molecules.

In this work, our main goal was to obtain the (frequency-independent) conductivity of two different fullerenol aqueous solutions $C_{60}(OH)_{22-26}$ (F1) and $C_{60}(OH)_{18-22}(OK)_4$ (F2), extracted from the measured bulk resistance, using the impedance spectroscopy technique, and explain its dependence upon the changing fullerenol concentration. In the low concentration region, it is expected that a linear dependence on ionic concentration should exist. Our efforts to explain the observed nonlinearities at higher concentrations by use of the Debye−Hückel and Onsager models are presented. With these results, it was possible to quantify the dissociation of the two distinct fullerenols investigated into fullerenol anions and H^+ (K^+) to determine the hydrodynamic radius and the dependence of the change of pH (and contra-ion K^+ concentration) as a function of the fullerenol molar concentration for aqueous solutions.

RESULTS

Following cell preparation, its impedance, covering the 10 kHz to 13 MHz range, was measured. A typical spectrum is shown in Figure 1, where both sets of data, modulus and phase angle, are presented. We were able to fit all data to an empirical impedance model consisting of dumped circuit elements describing a series circuit of the form[21]

$$Z(\omega) = \frac{1}{i\omega C_e + \sqrt{i\omega W_e} + R_e^{-1}} + \frac{1}{\sqrt{i\omega W_d} + R_d^{-1}} + \frac{1}{i\omega C_b + \sqrt{i\omega W_b} + R_b^{-1}} \quad (1)$$

In this model, the two first terms are relevant at low frequency values. The first one describes a double layer capacitance (C_e) in parallel to a Warburg impedance (W_e) and to an electrode resistance (R_e). It is followed by the second term presenting another Warburg impedance (W_d) in parallel to a frequency-independent element (R_d). The adjusted values for this parameter are concentration-dependent but not consistent with the expected bulk resistance at the nominal ionic concentration. It should properly be associated with a diffusion resistance effect.[22] This way, in the low frequency domain, electrode and diffusion effects are the contributions to the impedance spectrum. The last term is relevant to fit the spectrum at higher frequencies. The impedance modulus is characterized by a plateau, whereas the phase angle indicates values around zero. The value of the impedance in this region, almost given by its real part, is well represented by a

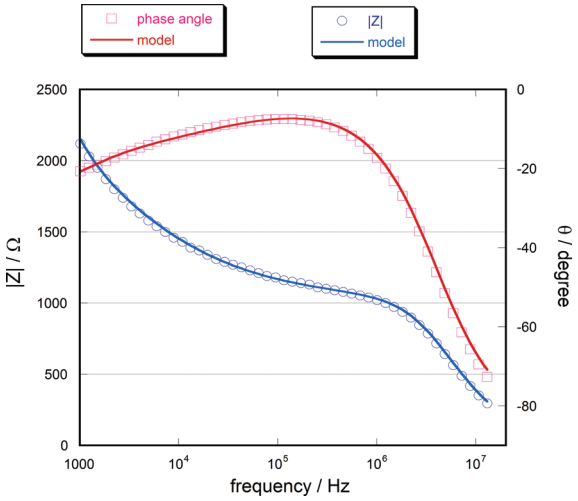

Figure 1. Impedance spectrum for the 1.2 kg/m^3 fullerenol type F1 solution. Symbols represent the experimental data; circles are the impedance modulus, and squares are the phase angle. Solid lines represent the fitting model. Parameters of eq 1 used in this fitting are $C_e = 1.4 \times 10^{-7}$ F, $W_e = 3 \times 10^{-8}\ \Omega^{-1}\ s^{-1/2}$, $R_e = 2 \times 10^3\ \Omega$, $W_d = 6.4 \times 10^{-6}\ \Omega^{-1}\ s^{-1/2}$, $R_d = 6.5 \times 10^3\ \Omega$, $C_b = 3.9 \times 10^{-11}$ F, $W_b = 1.4 \times 10^{-8}\ \Omega^{-1}\ s^{-1/2}$, $R_b = 1.2 \times 10^3\ \Omega$.

bulk resistance (R_b), defined by sample geometry and its conductivity.[21] At still higher frequencies, we can see a region of decreasing impedance modulus and also decreasing values of phase angle, which approach −90°. The value of the impedance associated with this spectral region is consistent with a bulk capacitance (C_b) having the dielectric constant of water. In order to get a better fitting quality, another Warburg element (W_b) was also necessary. As shown in Figure 1, fitting quality for both data sets, the modulus and phase angle of the measured impedance and over the whole measured spectral range, is good. This fitting quality was achieved on all measurements we have made.

Two samples of each fullerenol type have been prepared. Cell measurement reproducibility is better than 3%. Having values of bulk resistance R_b at hand, conductivity, as a function of fullerenol concentration, is readily obtained from the knowledge of cell geometry. For the fullerenol type F1, our conductivity data present an almost linear profile, whereas a strong nonlinear dependence was clearly observed for samples using the fullerenol type F2. These data are presented in Figure 2. In both cases, the first experimental point on the curve is the conductivity of water at zero fullerenol concentration. The solid lines in the graph are the adjusted theoretical curves using the model described below.

As given by its molecular formula, fullerenol type F1 presents no counterion besides hydrogen. It is expected that dissociated protons from the molecule and fullerenol anion are the only species present on these solutions. Evidence for hydrogen transport in compressed fullerenol powder has been investigated using impedance measurements[23,24] and confirmed

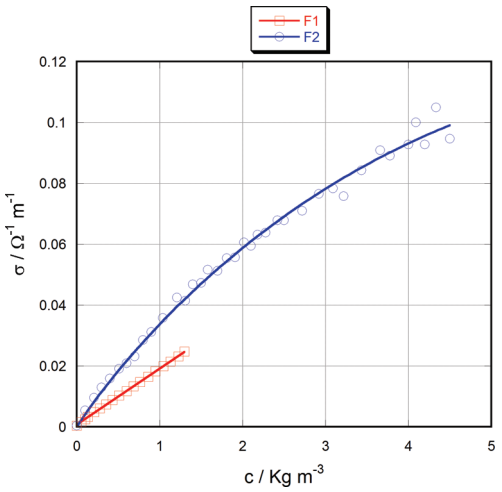

Figure 2. Conductivity of fullerenol sample as a function of concentration. Symbols represent the experimental data; squares are the conductivity data for the fullerenol type F1, and circles are the conductivity data for fullerenol type F2. Solid lines represent the fitting model.

by ESR measurements[12] in fullerenol aqueous solutions. In order to understand the conductivity of these solutions, we have assumed that the mobility of fullerenol anions is much smaller than proton mobility. Thus protons must be the dominant charge carriers forming the measured ionic current and sample conductivity can be written as

$$\sigma = \left[\frac{N_{av}10^3}{MW}\right]\mu_H \alpha e c \qquad (2)$$

where μ_H is proton mobility and we have used the standard value[25] $\mu_H = \mu_H^\circ = 3.63 \times 10^{-7} m^2\, s^{-1}\, V^{-1}$, e is the fundamental charge, N_{av} the Avogadro's number, MW the molecular weight of fullerenol given by its molecular formula, and c the nominal fullerenol concentration (kg/m^3). Parameter α gives the average number of protons that dissociates from the fullerenol molecule (its mean valence modulus). It is related to free proton concentration as $n_H = \alpha c$. Expected F1 type fullerenol molecular weight is 1128 g/mol given the contribution of 60 carbon atoms plus an average number of 24 OH groups attached to the molecule. Using this value, the obtained α parameter in the fitting procedure (shown in Figure 2) is 0.6.

Fullerenol type F2 presents a potassium counterion besides hydrogen, and its conductivity presents the nonlinear profile. This may indicate that mobility of fullerenol anions is relevant to transport processes. Its dissociation reaction is given by

$$C_{60}(OH)_M(OK)_N \rightarrow [C_{60}(OH)_{M-\alpha}(OK)_{N-\beta}O_{\alpha+\beta}]^{-(\alpha+\beta)} + \alpha H^+ + \beta K^+ \qquad (3)$$

The conductivity, depending on the three kinds of ions, the fullerenol anion, hydrogen, and potassium, is given by

$$\sigma = \left[\frac{eN_{av}10^3}{MW}\right](\mu_H z_H c_H + \mu_K z_K c_K + \mu_F z_F c_F) \qquad (4)$$

with indexes F, K, and H representing fullerenol, potassium, and hydrogen, respectively. There are some constrains imposed by the dissociation reaction and by the electroneutrality condition for eq 4 to hold, which are $c_H = \alpha c$, $c_K = \beta c$, and $c_F = c$. With the modulus of the valences given by $z_H = 1, z_K = 1$ and $z_F = \alpha + \beta$, eq 4 turns to

$$\sigma = \left[\frac{eN_{av}10^3}{MW}\right][\mu_H \alpha + \mu_K \beta + \mu_F(\alpha+\beta)]c \qquad (5)$$

The nonlinear effect could be associated with a concentration-dependent mobility. An empirical expression that accounts for this effect was first proposed by Kohlrausch[25] in the form $\mu_i = \mu_i^\circ - \lambda(c)^{1/2}$. In a later work, Debye and Hückel[26] showed that this formula could be understood in terms of ionic Coulombic interactions. Onsager made calculations,[27,28] valid for simple electrolytes, in a refinement of the Debye and Hückel theory. In a much more extensive work, Onsager and Fuoss[29] obtained an expression valid for an arbitrary number of ionic species. They showed that departure from linearity can be understood as a correction due to two mechanisms. One is derived from a drag force that a moving ion causes in another one of opposite sign and moving in opposite direction, and the other comes from a spatial offset between a moving ion and its accompanying ionic atmosphere.

The constant λ provided by Onsager and Fuoss[29] and adapted to fullerenol molecule is of the form

$$\lambda = \left[\frac{e}{6\pi\eta} + \left(\frac{h_1}{1+\sqrt{h_1}} + \frac{h_2}{1+\sqrt{h_2}}\right)\frac{eF\mu_F^\circ}{12\pi RT\varepsilon}\right] \times \sqrt{\frac{eFN_{av}10^3(\alpha+\beta)^4[\alpha+\beta+(\alpha+\beta)^2]}{RT\varepsilon[720+n+17\alpha+55\beta)]}}$$

$$h1 \equiv \frac{(\alpha+\beta)(\mu_K+\mu_F^\circ)}{(\alpha+\beta+1)[(\alpha+\beta)\mu_K+\mu_F^\circ]};$$

$$h2 \equiv \frac{(\alpha+\beta)(\mu_H+\mu_F^\circ)}{(\alpha+\beta+1)[(\alpha+\beta)\mu_H+\mu_F^\circ]} \qquad (6)$$

where η is the solvent viscosity, ε the dielectric constant of the solvent, T the temperature, F the Faraday constant, and R the universal gas factor. We also have written the molecular weight as MW = $720 + n + 17\alpha + 55\beta$, that is, the mass of 60 carbon atoms plus a number n that accounts for the mass of the nonsolvated groups in the molecule, the term 17α that accounts for the solvated α (O^-H^+) groups, and the term 55β that accounts for the solvated β (O^-K^+) groups. The first term in λ represents electrophoretic effects, the second and third terms (proportional to h_1 and h_2) describe the relaxation due to the spatial offset between the

moving hydrogen and potassium clouds and the fullerenol anions. We have shown[21] that conductivity of a KCl aqueous solution has a linear dependence over a wide range of ionic concentrations. In this sense, we assumed that potassium ions behave ideally even at the higher concentration values used here, presenting standard mobility equal to[25] $\mu_K = \mu_K^\circ = 7.62 \times 10^{-8}$ m^2 s^{-1} V^{-1}. For hydrogen mobility, we also assumed the standard mobility; likewise, we did in the linear conductivity, type F1 fullerenol case. Fullerenol mobility is written in the form

$$\mu_F = \mu_F^\circ - \lambda\sqrt{c} \quad (7)$$

Using eqs 5, 6, and 7, the concentration-dependent conductivity necessary to adjust F2 data in Figure 2 is written as

$$\sigma = \left[\frac{eN_{av}10^3}{720 + n + 17\alpha + 55\beta}\right][\mu_H\alpha + \mu_K\beta + (\mu_F^\circ - \lambda\sqrt{c})(\alpha + \beta)]c \quad (8)$$

This equation presents four constants determined through a fitting procedure, namely, the fullerenol standard ionic mobility μ_F°, the dissociation constants α and β, and the mass of nonsolvating groups n. Fitting results, shown in Figure 2, present a correlation factor greater than 0.98 and return the following parameter values $\mu_F^\circ = (2.0 \pm 0.5) \times 10^{-8}$ m^2 s^{-1} V^{-1}, $\alpha = (0.3 \pm 0.1)$, $\beta = (5.0 \pm 0.2)$, and $n = (3.9 \pm 0.7) \times 10^2$ atomic mass units.

DISCUSSION

Conductivity of type F1 fullerenol presented a linear dependence on concentration. At low concentration values, sample conductivity is nearly determined by an ionic mobility close to proton mobility. On the basis of this, we assumed a simple model in which protons dissociated from the molecule are the dominant charge carriers. In this case, we get an average number of dissociated protons per molecule equal to 0.6. Due to the high proton mobility, no information concerning fullerenol mobility was retrieved.

Samples containing type F2 fullerenol presented a nonlinear conductivity profile. In order to explain this effect, we have assumed that total sample mobility is the sum of potassium and hydrogen plus fullerenol ionic mobility, the latter being concentration-dependent, with correction terms given by the Debye–Hückel and Onsager theory. This way we get a four parameter fitting model that gives fullerenol mobility, potassium and hydrogen dissociation numbers, and molecular weight. Using the Stokes–Einstein relation, the obtained fullerenol mobility, and the mean valence $z_F = \alpha + \beta = 5.3 \pm 0.3$, a hydrodynamic radius of 2.0 ± 0.4 nm for fullerenol molecule was found. This radius is fairly consistent with a fullerene ball surrounded by a shell of molecular groups. It is also consistent with the existence of counterion interaction effects. The value of $\beta = 5$ found for the dissociation number of potassium is higher than the expected value from its molecular formula, equal to 4. As a consequence, we have found for the fullerenol molecular weight a value of 1390 ± 50 g/mol, which is consistent with the calculated value obtained by use of its molecular formula $\beta = 4$, equal to 1280 g/mol.

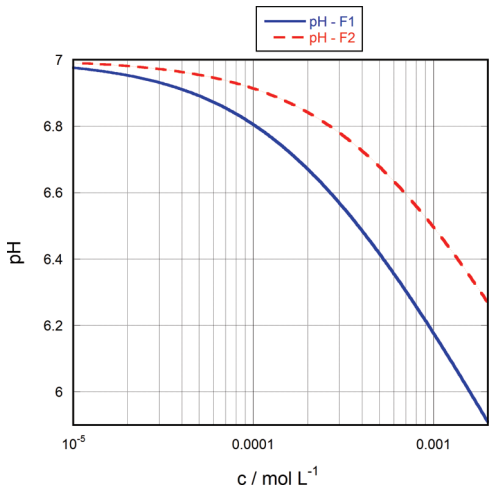

Figure 3. Expected pH calculated from conductivity data for type F1 fullerenol (solid line) and for type F2 fullerenol (dashed line).

The dissociation properties of the fullerenol molecule lead to a rise in proton concentration in the solution. This way a change in pH is expected and can be calculated using the relation

$$\mathrm{pH} = -\log\left(10^{-7} + \frac{\alpha c}{\mathrm{MW}}\right)$$

These pH values are shown in Figure 3 for both fullerenol types. Those changes may be useful in preparing fullerenol solutions for use in biochemistry experiments and pharmacological applications. For concentrations of about 0.1 mM, the fullerenol dissociation yields a pH change of about 0.1, while for about 2 mM, this change is about 1, which results in a pH of 6. A similar effect is expected for the dissociation of K^+ in the second fullerenol type.

CONCLUSION

This work has shown that impedance spectroscopy is a useful technique for investigating transport properties of solutions containing fullerene-derived molecules. For one of the two fullerenol types studied, high conductivity values were observed and explained in terms of hydrogen dissociation. For the other type, nonlinear effects in the conductivity were explained in terms of the Debye–Hückel and Onsager theory. In this case, interaction with counterions leads to a concentration-dependent ionic mobility. Values found for the fullerenol parameters are nearly consistent with those stated by

the manufacturer and with those found in the literature, validating the model presented here. In both cases, our conductivity model predicts that the fullerenol behaves as a weak acid and, thus, their hydrogen dissociation is capable of changing the pH of aqueous solutions.

METHODOLOGY

Two types of commercial fullerenol powder (Materials Technologies Research Ltd. http://www.mtr-ltd.com/Bio_Medicine.htm) were used in our experiments. Each experiment consisted of a measurement series ranging from high to low concentration values. High concentration samples were prepared by solvating them in deionized water, with precisely determined concentration values. In order to get best homogenization, these high concentration solutions were subjected to at least 15 min of a 40VA ultrasound bath. After the homogenization procedure, an open electrolytic cell was introduced into 1 mL of each of the high concentration solutions. This way solution volume completely fulfilled the cell and its surroundings. This procedure allowed us to easily change concentration values by just adding deionized water into the solution volume. We have checked, using standard salt solutions, that the cell correctly presents a linear conductivity profile upon the changing salt concentration. This open cell was built in parallel plate geometry using stainless steel electrodes, without a guard ring. Electrode area, having 35 mm^2, was separated by 1 mm. The open cell configuration has the advantage of best control of concentration values by use of sequential dilutions. In order to take into account the lack of a guard ring, a precise calibration using standard NaCl solutions and an open cell, also without a guard ring, and of very large geometric factor (941 mm), defined as the area/separation ratio, was made. It resulted in measured mobility values close to published ones within 2.5%. In sequence, we made simultaneous measurements using both cells in the same calibrated solution. Comparison of the measured conductivities led to an effective area value of 44 mm^2 for the cell used in the experiments. This value was keep as the effective cell area in the analysis of the data. Before each experiment, the conductivity of the deionized water used to prepare the fullerenol solutions was measured using the method described above. We assured its conductivity would fall below 150 μS/m. According to the manufacturer's Web site, molecular formulas for the two commercial types used are $[C_{60}(OH)_{22-26}]$ and $[C_{60}(OH)_{18-22}(OK)_4]$. Concentration of the fullerenol solutions spanned an interval of 0.1 to 1.5 kg/m^3 of powder in water for fullerenol type F1 and 0.1 to 4.5 kg/m^3 for fullerenol type F2. Higher concentration values were used for the case of type F2 fullerenol because of its much higher solubility.

Acknowledgment. This work was funded by FAPEMIG, CNPq, and the INCT Nanomateriais de Carbono.

REFERENCES AND NOTES

1. Kroto, H. W.; Heath, J. R.; O'Brien, S. C.; Curl, R. F.; Smalley, R. E. C_{60}: Buckminsterfullerene. *Nature* **1985,** *318*, 162–163.
2. Krätschmer, W.; Fostiropoulos, K.; Huffman, D. R. The Infrared and Ultraviolet Absorption Spectra of Laboratory-Produced Carbon Dust: Evidence for the Presence of the C_{60} Molecule. *Chem. Phys. Lett.* **1990,** *170*, 167–170.
3. Reyes-Reyes, M.; Kim, K.; Carroll, D. L. High-Efficiency Photovoltaic Devices Based on Annealed Poly(3-hexylthiophene) and 1-(3-Methoxycarbonyl)-propyl-1-phenyl-(6,6)C_{61} Blends. *Appl. Phys. Lett.* **2005,** *87*, 1–3.
4. Park, J. W.; Pasupathy, A. N.; Goldsmith, J. I.; Soldatov, A. V.; Chang, C.; Yaish, Y.; Sethna, J. P.; Abruna, H. D.; Ralph, D. C.; McEuen, P. L. Wiring up Single Molecules. *Thin Solid Films* **2003,** *438*, 457–461.
5. Harneit, W. Fullerene-Based Electron-Spin Quantum Computer. *Phys. Rev. A* **2002,** *65*, 1–6.
6. Bosi, S.; Da Ros, T.; Spalluto, G.; Prato, M. Fullerene Derivatives: An Attractive Tool for Biological Applications. *Eur. J. Med. Chem.* **2003,** *38*, 913–923.
7. Nakamura, E.; Isobe, H. Functionalized Fullerenes in Water the First 10 Years of Their Chemistry, Biology, and Nanoscience. *Acc. Chem. Res.* **2003,** *36*, 807–815.
8. Li, J.; Takeuchi, A.; Ozawa, M.; Li, X.; Saigo, K.; Kitazawa, K. C_{60} Fullerol Formation Catalysed by Quaternary Ammonium Hydroxides. *J. Chem. Soc., Chem. Commun.* **1993,** *23*, 1784–1785.
9. Li, T.; Li, X.; Huang, K.; Jiang, H.; Li, J. Synthesis and Characterization of Hydroxylated Fullerene Epoxide: An Intermediate for Forming Fullerol. *J. Cent. South Univ. Technol. (Engl. Ed.)* **1999,** *6*, 35–36.
10. Gonzalez, K. A.; Wilson, L. J.; Wu, W.; Nancollas, G. H. Synthesis and *In Vitro* Characterization of a Tissue-Selective Fullerene: Vectoring $C_{60}(OH)_{16}$AMBP to Mineralized Bone. *Bioorg. Med. Chem.* **2002,** *10*, 1991–1997.
11. Husebo, L. O.; Sitharaman, B.; Furukawa, K.; Kato, T.; Wilson, L. J. Fullerenols Revisited as Stable Radical Anions. *J. Am. Chem. Soc.* **2004,** *126*, 12055–12064.
12. Zhang, J.-M.; Yang, W.; He, P.; Zhu, S.-Z. Efficient and Convenient Preparation of Water-Soluble Fullerenol. *Chin. J. Chem.* **2004,** *22*, 1008–1011.
13. Alves, G. C.; Ladeira, L. O.; Righi, A.; Krambrock, K.; Calado, H. D.; Gil, R.; Pinheiro, M. V. B. Synthesis of $C_{60}(OH)_{18-20}$ in Aqueous Alkaline Solution under O_2-Atmosphere. *J. Braz. Chem. Soc.* **2006,** *17*, 1186–1190.
14. Mirkov, S. M.; Djordjevic, A. N.; Andric, N. L.; Andric, S. A.; Kostic, T. S.; Bogdanovic, G. M.; Vojinovic-Miloradov, M. B.; Kovacevic, R. Z. Nitric Oxide-Scavenging Activity of Polyhydroxylated Fullerenol, $C_{60}(OH)_{24}$. *Nitric Oxide* **2004,** *11*, 201–207.
15. Djordjevic, A.; Canadanovic-Brunet, J.; Vojinovic-Miloradov, M.; Bogdanovic, G.; Cebovic, T. ESR Study of Antioxidative Mechanism of Fullerol. *Free Radical Res.* **2003,** *37*, 63.
16. Yin, J.-J.; Lao, F.; Fu, P. P.; Wamer, W. G.; Zhao, Y. L.; Wang, P. C.; Qiu, Y.; Sun, B. Y.; Xing, G. M.; Dong, J. Q.;*et al.*The Scavenging of Reactive Oxygen Species and the Potential for Cell Protection by Functionalized Fullerene Materials. *Biomaterials* **2009,** *30*, 611–621.
17. Dugan, L. L.; Gabrielsen, J. K.; Yu, S. P.; Lin, T.-S.; Choi, D. W. Buckminsterfullerenol Free Radical Scavengers Reduce Excitotoxic and Apoptotic Death of Cultured Cortical Neurons. *Neurobiol. Dis.* **1996,** *3*, 129–135.
18. Lai, H. S.; Chen, Y.; Chen, W. J.; Chang, K. J.; Chiang, L. Y. Free Radical Scavenging Activity of Fullerenol on Grafts after Small Bowel Transplantation in Dogs. *Transplant. Proc.* **2000,** *32*, 1272–1274.
19. Dragojevic-Simic, V.; Jacevic, V.; Dobric, S.; Djordjevic, A.; Djordjevic-Milic, V.; Trajkovic, S.; Milosavljevic, I. Protective Effects of Fullerenol $C_{60}(OH)_{24}$ against Doxorubicin and Whole-Body Radiation-Induced Toxicity in Rats. *Toxicol. Lett.* **2008,** *180*, S221–S221.
20. Bogdanovic, V.; Stankov, K.; Icevic, I.; Zikic, D.; Nikolic, A.; Solajic, S.; Djordjevic, A.; Bogdanovic, G. fullerenol C_{60}-$(OH)_{24}$ Effects on Antioxidative Enzymes Activity in Irradiated Human Erythroleukemia Cell Line. *J. Radiat. Res.* **2008,** *49*, 321–327.
21. Sardenberg, R.; Figueiredo, J. M. A. Relationship between Spatial and Spectral Properties of Ionic Solutions: The Distributed Impedance of an Electrolytic Cell. *Electrochim. Acta* **2010,** *55*, 4722–4727.
22. Jamnik, J.; Maier, J. Generalised Equivalent Circuits for Mass and Charge Transport: Chemical Capacitance and

Its Implications. *Phys. Chem. Chem. Phys.* **2001,** *3*, 1668–1678.
23. Hinokuma, K.; Ata, M. Fullerene Proton Conductors. *Chem. Phys. Lett.* **2001,** *341*, 442–446.
24. Hinokuma, K.; Ata, M. Proton Conduction in Polyhydroxy Hydrogensulfated Fullerenes. *J. Electrochem. Soc.* **2003,** *150*, A112–A116.
25. Oldham, K. B.; Myland, J. C. *Fundamentals of Electrochemical Science*; Academic Press: New York, 1994.
26. Debye, P.; Hückel, E. The Theory of Electrolytes. I. Lowering of Freezing Point and Related Phenomena. *Z. Phys. Chem.* **1923,** *24*, 185–206.
27. Onsager, L. Zur Theorie der Elektrolyte. I. *Z. Phys. Chem.* **1926,** *27*, 388–392.
28. Onsager, L. Zur Theorie der Elektrolyte. II. *Z. Phys. Chem.* **1927,** *28*, 277–298.
29. Onsager, L.; Fuoss, R. M. Irreversible Processes in Electrolytes. Diffusion, Conductance and Viscous Flow in Arbitrary Mixtures of Strong Electrolytes. *J. Phys. Chem.* **1932,** *36*, 2689–2778.